

Electronic structure of $\text{CaCu}_3\text{Ru}_4\text{O}_{12}$ studied by x-ray photoemission spectroscopy

T. T. Tran,¹ K. Takubo,¹ T. Mizokawa,^{1,2} W. Kobayashi,³ and I. Terasaki^{3,4}

¹Department of Physics and Department of Complexity Science and Engineering, University of Tokyo, Chiba 277-8581, Japan

²PRESTO, Japan Science and Technology Agency, 4-1-8 Honcho Kawaguchi, Saitama, Japan

³Department of Applied Physics, Waseda University, Tokyo 169-8555, Japan

⁴CREST, Japan Science and Technology Agency, Tokyo 108-0075, Japan

(Received 3 July 2005; revised manuscript received 22 February 2006; published 17 May 2006)

We have studied the electronic structure of the d -electron heavy-fermion system $\text{CaCu}_3\text{Ru}_4\text{O}_{12}$ using x-ray photoemission spectroscopy and a cluster model calculation. The Ru $3d$ core level spectrum shows a double-peak structure as commonly observed in metallic Ru oxides. In $\text{CaCu}_3\text{Ru}_4\text{O}_{12}$, the well-screened peak has dominating intensity, indicating that the Ru $4d$ electrons in $\text{CaCu}_3\text{Ru}_4\text{O}_{12}$ are highly itinerant. On the other hand, the Cu $2p_{3/2}$ core level peak is accompanied by a satellite and shows that the valence state of Cu is close to $3d^9$ (Cu^{2+}) with localized character. In addition, the main Cu $2p_{3/2}$ peak shows an asymmetric line shape due to the screening effect, suggesting the hybridization effect between the Cu $3d$ and Ru $4d$ orbitals. The present results show that, among the d -electron heavy-fermion materials, the electronic structure of $\text{CaCu}_3\text{Ru}_4\text{O}_{12}$ best resembles that of the f -electron Kondo system.

DOI: 10.1103/PhysRevB.73.193105

PACS number(s): 71.27.+a, 79.60.-i, 71.28.+d

Research on heavy-fermion materials was started by the discovery of an enormous electronic heat capacity coefficient in CeAl_3 ,¹ and has been accelerated by the discovery of superconductivity in CeCu_2Si_2 ,² and recently by observations of heavy-fermion behavior in transition-metal oxides.³ While in f -electron heavy-fermion compounds the Kondo lattice model gives the essentials of the underlying physics, the routes to the formation of heavy quasiparticle masses would be very different in transition-metal oxides. This makes research on d -electron heavy-fermion systems a hot topic in strongly correlated material science and attracts the interest of many researchers, both experimentalists and theoreticians.³

$\text{CaCu}_3\text{Ru}_4\text{O}_{12}$ is a newly discovered d -electron heavy-fermion system⁴ in which a transport study indicates that the heavy-fermion behavior comes from the Kondo mechanism just as in an f -electron heavy-fermion system. In this scenario, Cu $3d$ and Ru $4d$, respectively, play the roles of the localized f electron and the conduction electron. This point makes $\text{CaCu}_3\text{Ru}_4\text{O}_{12}$ different from other d -electron heavy-fermion systems, such as LiV_2O_4 , in which only V $3d$ electrons have important roles.⁵ $\text{CaCu}_3\text{Ru}_4\text{O}_{12}$ has the perovskite-type crystal structure as shown in Fig. 1. While the Ca and Cu ions occupy the A site coordinated by the 12 oxygen ions, the Ru ions occupy the B site octahedrally coordinated by the six oxygen ions. The corner-sharing Ru-O network is expected to provide a relatively wide Ru $4d$ -O $2p$ band near the Fermi level just as in other perovskite-type Ru oxides such as SrRuO_3 and Sr_2RuO_4 . On the other hand, the hybridization between the Cu $3d$ and O $2p$ orbitals would be different from that in typical perovskite-type Cu oxides such as LaCuO_3 and La_2CuO_4 . In our experiment, we examine the electronic structure of $\text{CaCu}_3\text{Ru}_4\text{O}_{12}$ by x-ray photoemission spectroscopy (XPS), in order to get information about the above scenario.

Our XPS measurements were carried out at room temperature using JPS9200 spectrometer. Monochromatic $\text{AlK}\alpha$ (1486.6 eV) was used as an x-ray source. The pass energy of

the electron analyzer was set to 10 eV. The total energy resolution including the x-ray source and the electron analyzer was about 0.6 eV. The binding energy was calibrated using the Fermi edge and the Au $4f$ core level (84.0 eV) of the gold reference sample. The polycrystalline samples of $\text{CaCu}_3\text{Ru}_4\text{O}_{12}$ prepared by a solid-state reaction were fractured *in situ* to obtain a clean surface. The base pressure of the chamber was 7×10^{-8} Pa.

Figure 2 shows the valence band XPS spectrum of $\text{CaCu}_3\text{Ru}_4\text{O}_{12}$. Three main structures (A, B, and C) were observed. Compared with the XPS result for Sr_2RuO_4 and its analysis,⁶ we can conclude that the peak at around -0.8 eV (structure C) and the broad structure at around -6 eV (structure A) are derived from, respectively, the Ru $4d_{t_{2g}}$ band (hybridized with the O $2p$ states) and the O $2p$ band (hybridized with the Ru $4d$ states). Therefore, structure B, which does not appear in the spectrum of Sr_2RuO_4 , is mainly constructed from the Cu $3d$ states. The Cu $3d$ band is located at ~ -2.5 eV. In the case of CuO, the main Cu $3d$ band is located at ~ -3.1 eV and the Zhang-Rice singlet level with the 1A_1 symmetry is located at ~ -1.3 eV.^{7,8} Assuming that the

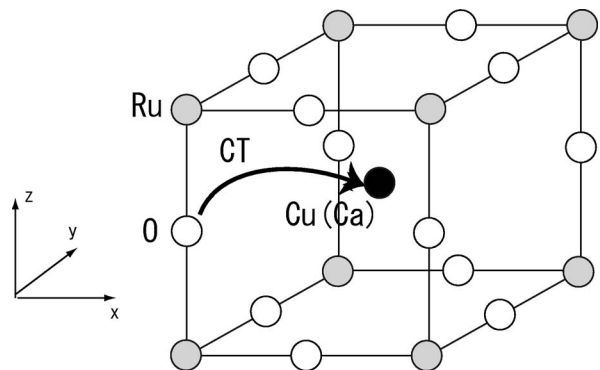


FIG. 1. Schematic drawing of the crystal structure of $\text{CaCu}_3\text{Ru}_4\text{O}_{12}$. The arrow indicates the charge transfer from the O $2p$ to Cu $3d$ orbitals.

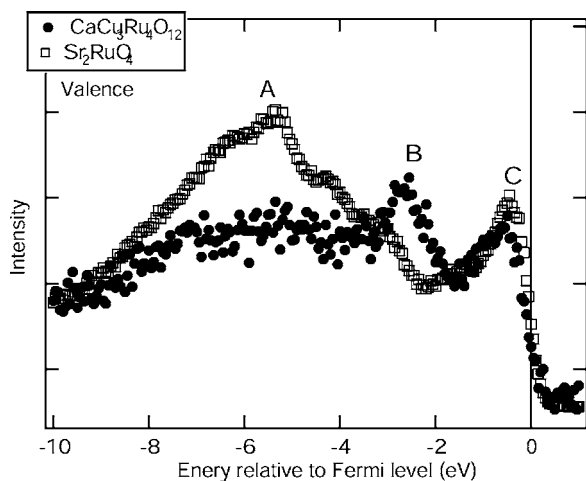


FIG. 2. Valence band XPS spectra of $\text{CaCu}_3\text{Ru}_4\text{O}_{12}$ (closed circles) and Sr_2RuO_4 (open squares).

energy separation between the main Cu 3d band and the Zhang-Rice singlet level in $\text{CaCu}_3\text{Ru}_4\text{O}_{12}$ is comparable or smaller than CuO, the Zhang-Rice singlet level does not reach the Fermi level. This assumption is reasonable since the Cu 3d–O 2p hybridization of $\text{CaCu}_3\text{Ru}_4\text{O}_{12}$ is rather weak compared to that of CuO, as indicated from the cluster model analysis of the Cu 2p spectra. Therefore, the electronic states at the Fermi level is dominated by the Ru $4d_{t_2g}$ states and the Zhang-Rice singlet level derived from the Cu 3d states is buried in the Ru $4d_{t_2g}$ band. Therefore, in the ground state, the Cu ion takes the d^9 electronic configuration with localized spin 1/2. The Zhang-Rice singlet state is the final state of the photoemission process from this d^9 ground state. As shown in Fig. 2, the Ru $4d_{t_2g}$ bandwidth and the density of states at the Fermi level in $\text{CaCu}_3\text{Ru}_4\text{O}_{12}$ are similar to those in Sr_2RuO_4 . The high density of states near the Fermi level is the origin of the strong screening effects on core holes as discussed below.

The Ru 3d core level XPS result for $\text{CaCu}_3\text{Ru}_4\text{O}_{12}$ is shown in Fig. 3 together with the same result in Sr_2RuO_4 . Both spectra show a clear double-peak structure which can be assigned as poorly screened (A) and well-screened (B) peaks due to the screening effect of the conduction electrons.¹⁴ The theory states that satellite structure may occur when the core-valence Coulomb interaction is strong enough to form well-screened and poorly screened final states. The main and satellite structures correspond to the well-screened and poorly screened final states, respectively. In metallic Ru oxides such as SrRuO_3 and Sr_2RuO_4 , the intensity of the well-screened peak is dominant while the intensity of the poorly screened peak becomes dominant in insulating Ru oxides such as Ca_2RuO_4 .^{9–11} In $\text{CaCu}_3\text{Ru}_4\text{O}_{12}$, the intensity of the well-screened peak is more dominant than those in SrRuO_3 and Sr_2RuO_4 and is comparable to that in RuO_2 ,¹² indicating that the Ru 4d electrons in $\text{CaCu}_3\text{Ru}_4\text{O}_{12}$ are much more itinerant than those in SrRuO_3 and Sr_2RuO_4 . Since the screening process of the Ru 3d core level involves the extended Ru 4d electrons, quantitative analysis of the Ru 3d spectrum is very difficult. It would be interesting to develop a new theoretical method to analyze

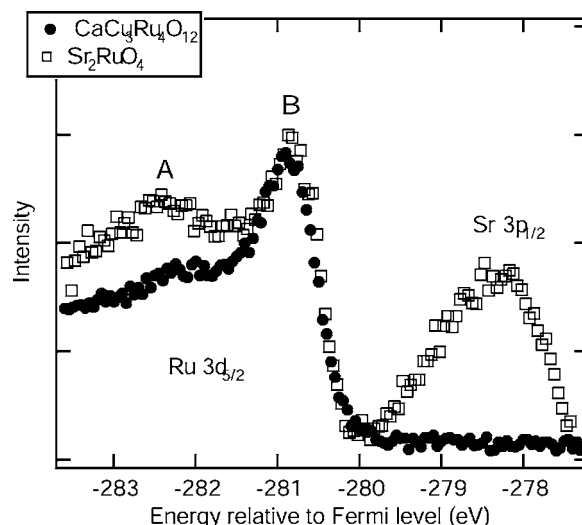


FIG. 3. Ru 3d core level XPS spectra of $\text{CaCu}_3\text{Ru}_4\text{O}_{12}$ (closed circles) and Sr_2RuO_4 (open squares).

the Ru 3d spectrum of the metallic Ru oxides. For example, Anderson impurity model would be useful to analyze the Ru 3d spectrum as applied to the Cu 2p spectrum by Koitzsch and co-workers.¹³

Figure 4 shows XPS result for the Cu $2p_{3/2}$ core level. It shows the satellite structure (A) and the main peak (C). A shoulder structure (B) of the main peak is also observed. The satellite structure is commonly observed in insulating transition-metal oxides such as CuO and NiO. The existence of the satellite structure shows that the Cu 3d level is partially filled and that the O 2p electrons can be transferred to the empty Cu 3d orbitals to screen the Cu 2p core hole. In addition, the line shape of the satellite structure is similar to those observed in Cu^{2+} oxides such as CuO and La_2CuO_4 . Therefore, it is reasonable to conclude that the valence state of Cu is close to $3d^9$ (Cu^{2+}) and that the Cu 3d electrons in this system are almost localized. In order to confirm this interpretation, we have analyzed the main and satellite structures using the configuration interaction calculation on the CuO_{12} cluster model (see Fig. 1).^{15,17,18} In this description,

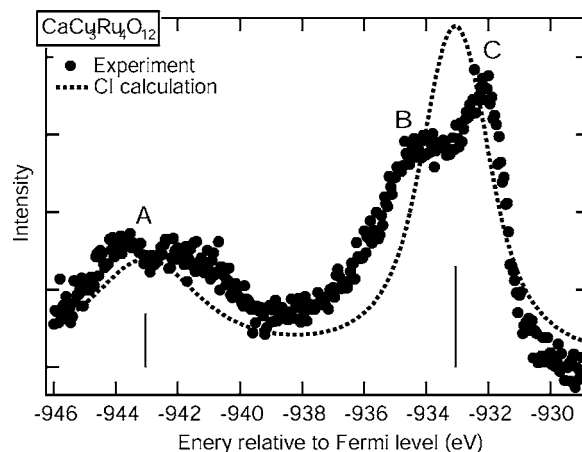


FIG. 4. Cu 2p photoemission spectrum of $\text{CaCu}_3\text{Ru}_4\text{O}_{12}$ (closed circles) and the cluster model analysis (dotted curve).

the ground state is given by the linear combination of $3d^9$ and $3d^{10}\underline{L}$ states:

$$\Psi_g = \alpha_1|d^9\rangle + \alpha_2|d^{10}\underline{L}\rangle, \quad (1)$$

where d implies a Cu $3d$ electron and \underline{L} denotes an O $2p$ ligand hole. The final states are given by the linear combinations of $\underline{c}3d^9$ and $\underline{c}3d^{10}\underline{L}$ where c represents the Cu $2p_{3/2}$ core hole:

$$\Psi_f = \beta_1|\underline{c}d^9\rangle + \beta_2|\underline{c}d^{10}\underline{L}\rangle. \quad (2)$$

Adjustable parameters are the charge-transfer energy from the O $2p$ orbitals to the empty Cu $3d$ orbitals, Δ , the Coulomb interaction between the Cu $3d$ electron and the Cu $2p$ core hole, Q , and the transfer integrals between the Cu $3d$ and O $2p$ orbitals, which can be expressed by Slater-Koster parameters ($pd\pi$) and ($pd\sigma$). Here, the ratio ($pd\sigma$)/($pd\pi$) is -2.2 . The energy difference between the $3d^9$ and $3d^{10}\underline{L}$ states is given by Δ and that between the $\underline{c}3d^9$ and $\underline{c}3d^{10}\underline{L}$ by $\Delta - Q$. The hybridization term between the $3d^9$ ($\underline{c}3d^9$) and $3d^{10}\underline{L}$ ($\underline{c}3d^{10}\underline{L}$) states is given by the transfer integrals. The calculated Cu $2p$ core level photoemission spectrum is broadened with an energy-dependent Lorentzian such that the Lorentzian full width at half maximum is

$$2\Gamma = 2\Gamma_0(1 + \alpha\Delta E), \quad (3)$$

where Γ_0 and Γ are, respectively, the lifetime broadening of the main and satellite peaks, ΔE denotes the energy separation from the main peak, while α is the broadening parameter. We adopted the values $\Gamma_0=1.0$ eV and $\alpha=0.1$.¹⁷ The Gaussian broadening of 1.0 eV is also used for the entire spectrum to simulate the instrumental resolution and other broadening effects. We have obtained the best-fit result by setting $Q=10.0$ eV, $\Delta=0.2$ eV, and ($pd\sigma$)= -1.0 eV. Since the charge transfer energy $\Delta=0.2$ is smaller than the Coulomb interaction between the Cu $3d$ electron and the Cu $2p$ core hole, Q , the satellite structure in Cu $2p$ spectra has $\underline{c}3d^9$ character and the main peak has $\underline{c}3d^{10}\underline{L}$ character. The transfer integral between the Cu $3d$ and O $2p$ orbitals is much smaller than those reported for CuO and La_2CuO_4 .^{8,17,18} This is consistent with the fact that the Cu ions occupy A site of the perovskite lattice. The charge transfer energy Δ is also smaller than those reported for the Cu^{2+} oxides.^{17,18} While the smallness of transfer integral tends to make the Cu $3d$ electrons in the present system more localized than those in La_2CuO_4 or Nd_2CuO_4 , the smallness of the charge-transfer energy tends to make the Cu $3d$ electrons in the present system more delocalized than those in La_2CuO_4 or Nd_2CuO_4 . Probably these two effects cancel with each other to some extent and the localization of the Cu $3d$

electrons in $\text{CaCu}_3\text{Ru}_4\text{O}_{12}$ would be more or less similar to that in La_2CuO_4 or Nd_2CuO_4 .

The calculated result is plotted in Fig. 4. We could not reproduce the shoulder structure of the main peak since we employed the single-site cluster model in our calculation. The shoulder structure (B) of the main peak is caused by the nonlocal screening mechanism:¹⁶ screening by transferring an electron from the outside of the CuO_{12} cluster considered above. In the present system, the nonlocal screening due to the Ru $4d$ electrons is expected to be dominant since the Ru $4d$ density of states at the Fermi level is considerably high. Recently, an x-ray absorption study has shown that the Cu valence in $\text{CaCu}_3\text{Ti}_4\text{O}_{12}$ is also $+2$.¹⁹ However, it is expected that the nonlocal screening channel is almost suppressed in $\text{CaCu}_3\text{Ti}_4\text{O}_{12}$ where the Ti $3d$ orbitals are unoccupied and the Cu ion is essentially isolated.

The Cu $2p$ spectrum with the satellite structure indicates that the Cu $3d$ electrons are relatively localized in contrast to the itinerant Ru $4d$ electrons. In this sense, the electronic structure of $\text{CaCu}_3\text{Ru}_4\text{O}_{12}$ is rather similar to that of $4f$ -electron heavy-fermion materials in which the highly localized $4f$ electrons hybridize with the conduction electrons. However, the asymmetric line shape of the Cu $2p$ main peak indicates that the Ru $4d$ -Cu $3d$ screening channel is very active to screen the Cu $2p$ core hole. Actually, the cluster model analysis of the Cu $2p$ spectrum shows that the transfer integral between the Cu $3d$ and O $2p$ orbitals is as large as ~ 1 eV and the Ru $4d$ -Cu $3d$ hybridization via the O $2p$ orbitals is expected to large compared with the $4f$ -electron heavy-fermion systems. Here, one can speculate that the Cu $3d$ electrons would be less localized than the $4f$ -electron systems and would be comparable to the $5f$ -electron systems. In future, further experiments should be performed on $\text{CaCu}_3\text{Ru}_4\text{O}_{12}$ to reveal to what extent the Kondo picture can be applicable to $\text{CaCu}_3\text{Ru}_4\text{O}_{12}$. One of the most important experiments is the photoemission spectroscopy experiment with high-energy resolution in which one would observe a Kondo peak at the Fermi level.

In conclusion, we have performed the XPS measurement of $\text{CaCu}_3\text{Ru}_4\text{O}_{12}$. The Ru $3d$ spectrum indicates that Ru $4d$ electrons are highly itinerant while Cu $2p$ spectrum reveals the localization of Cu $3d$ electrons. This supports the scenario which Kobayashi *et al.* proposed about the mechanism of the heavy-fermion behavior in $\text{CaCu}_3\text{Ru}_4\text{O}_{12}$ and shows that, among the d -electron heavy-fermion materials, the electronic structure of $\text{CaCu}_3\text{Ru}_4\text{O}_{12}$ best resembles that of the f -electron Kondo system.

This work was supported by the Ministry of Education, Culture, Sports, Science and Technology of Japan.

¹K. Andres, J. E. Graebner, and H. R. Ott, Phys. Rev. Lett. **35**, 1779 (1975). Friday, March 31, 2006 at 14:08

²F. Steglich, J. Aarts, C. D. Bredl, W. Lieke, D. Meschede, W. Franz, and H. Schafer, Phys. Rev. Lett. **43**, 1892 (1979); G. R.

Steward, Rev. Mod. Phys. **56**, 755 (1984).

³T.-A. Krug von Nidda, R. Bulla, N. Buttgen, M. Heinrich, and A. Loidl, Eur. Phys. J. B **34**, 399 (2003).

⁴W. Kobayashi, I. Terasaki, J. Takeya, I. Tsukuda, and Y. Ando, J.

- Phys. Soc. Jpn. **73**, 2373 (2004).
- ⁵S. Kondo, D. C. Johnston, C. A. Swenson, F. Borsa, A. V. Mahajan, L. L. Miller, T. Gu, A. I. Goldman, M. B. Maple, D. A. Gajewski, E. J. Freeman, N. R. Dilley, R. P. Dickey, J. Merrin, K. Kojima, G. M. Luke, Y. J. Uemura, O. Chmaissem, and J. D. Jorgensen, Phys. Rev. Lett. **78**, 3729 (1997).
- ⁶T. T. Tran, T. Mizokawa, S. Nakatsuji, H. Fukazawa, and Y. Maeno, Phys. Rev. B **70**, 153106 (2004).
- ⁷J. Ghijsen, L. H. Tjeng, J. van Elp, H. Eskes, J. Westerink, G. A. Sawatzky, and M. T. Czyzyk, Phys. Rev. B **38**, 11322 (1988).
- ⁸H. Eskes, L. H. Tjeng, and G. A. Sawatzky, Phys. Rev. B **41**, 288 (1990).
- ⁹P. A. Cox, R. G. Egdell, J. B. Goodenough, A. Hamnett, and C. C. Naish, J. Phys. C **16**, 6221 (1983).
- ¹⁰A. Sekiyama, S. Kasai, M. Tsunekawa, Y. Ishida, M. Sing, A. Irizawa, A. Yamasaki, S. Imada, T. Muro, Y. Saito *et al.*, Phys. Rev. B **70**, 060506(R) (2004), and unpublished results.
- ¹¹T. T. Tran, T. Mizokawa, S. Hirata, K. Takubo, M. Kurokawa, H. Yagi, A. Fujimori, S. Nakatsuji, H. Fukazawa, and Y. Maeno (unpublished).
- ¹²Y. Kaga, Y. Abe, H. Yanagisawa, M. Kawamura, and K. Sasaki, Surf. Sci. Spectra **6**, 68 (1999).
- ¹³A. Koitzsch, J. Fink, M. S. Golden, K. Karlsson, O. Jepsen, O. Gunnarsson, L. L. Miller, H. Eisaki, S. Uchida, G. Yang, and S. Abell, Phys. Rev. B **66**, 024519 (2002).
- ¹⁴A. Kotani and Y. Toyazawa, J. Phys. Soc. Jpn. **37**, 912 (1974).
- ¹⁵Stefan Hufner, *Photoelectron Spectroscopy* (Springer, Berlin, 2003).
- ¹⁶M. A. van Veenendaal and G. A. Sawatzky, Phys. Rev. Lett. **70**, 2459 (1993); Phys. Rev. B **49**, 3473 (1994).
- ¹⁷A. E. Bocquet, T. Mizokawa, T. Saitoh, H. Namatame, and A. Fujimori, Phys. Rev. B **46**, 3771 (1992).
- ¹⁸K. Okada and A. Kotani, J. Phys. Soc. Jpn. **58**, 2578 (1989).
- ¹⁹C. McGuinness, J. E. Downes, P. Sheridan, P.-A. Glans, K. E. Smith, W. Si, and P. D. Johnson, Phys. Rev. B **71**, 195111 (2005).